CRYSTAL GROWTH & DESIGN

Article

pubs.acs.org/crystal

Generalized Synthesis of Calixarene-Based High-Nuclearity M_{4n} Nanocages (M = Ni or Co; n = 2−6)

Published as part of the Crystal Growth & Design virtual special issue IYCr 2014 - Celebrating the International Year of Crystallography.

Kongzhao Su,[†,§] Feilong Jiang,[†] Jinjie Qian,[†,§] Yanli Gai,[†,§] Mingyan Wu,[†] Salem M. Bawaked,[‡] Mohamed Mokhtar,[‡] Shaeel A. AL-Thabaiti,[‡] and Maochun Hong*[,†]

[†]State Key Laboratory of Structural Chemistry, Fujian Institute of Research on the Structure of Matter, Chinese Academy of Sciences, Fuzhou 350002, China

[‡]Department of Chemistry, Faculty of Science, King Abdulaziz University, Jeddah 21589, Saudi Arabia

[§]University of the Chinese Academy of Sciences, Beijing 100049, China

Supporting Information

ABSTRACT: A family of high-nuclearity M_{4n} (M = Ni or Co, n = 2−6) coordination nanocages constructed by M_4−calix[4]arene molecular building blocks (MBBs) with inorganic phosphate or organic phosphonate ligands have been isolated by solvothermal syntheses and characterized by single-crystal X-ray diffraction. This family can be divided into five structural types with an increase in the number of M_4−calix[4]arene MBBs, including Ni_8 (**1** and **2**, n = 2), M_{12} (M = Ni (**3**) and Co (**4**), n = 3), M_{16} (M = Ni (**5**) and Co (**6**), n = 4), Co_{20} (**7**, n = 5), and Co_{24} (**8**, n = 6) coordination nanocages. Structural analyses reveal that the metallic cores of **1** and **2** are arranged in chair conformation, while compounds **3**−**6** with closed-shell structures, where their ports are sealed by sodium ions, present the first examples of 2p-3d heterometallic metal−calixarene nanocages to our knowledge. The novel helmet-like Co_{20} (**7**) is the only one in this family with an open-shell structure, which can be thought of as a truncated octahedral Co_{24} (**8**) nanocage cutting one face. Furthermore, the magnetic behaviors of **1**−**8** have been investigated, suggesting the existence of strong antiferromagnetic interactions between magnetic centers for all title coordination cages.

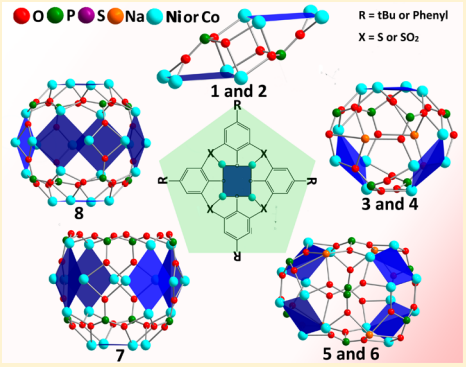

INTRODUCTION

High-nuclearity coordination cage complexes is one of the most fascinating research fields emerging in the past two decades not only because of their intriguing architectures, compositional diversity, and interesting properties[1] but also their applications such as gas storage and separation,[2] encapsulation of various guests,[3] materials as effective catalyst for organic species,[4] and so on.[5] So far, a variety of coordination cages with different nuclearities and shapes as well as cavities have been reported.[6] However, the rational design and systematic synthesis of novel polynuclear cage compounds is still filled with challenges in coordination chemistry. In recent years, one route to reach the above-mentioned goal is to search a library of complexes and exploit the known coordination modes of certain ligands. Thereafter, polynuclear cage compounds can be made through the self-assembly of complementary ligands with the preferred coordination modes by means of logical or multistep procedures.[7] Thus, it is very critical to choose appropriate ligands in polynuclear cage compound formation.

A family of ligands that have recently been employed in synthesizing polymetallic complexes, in ours as well as other groups, are calixarenes. Calixarenes, as a bowl-shaped macrocyclic ligand linked by methylene, sulfur, or other heteroatom bridges with hydroxyl groups at the lower rim, have been proved to be excellent ligands to construct polymetallic compounds.[8] In the past few years, we (among others) found that one thiacalix[4]arene or sulfonylcalix[4]arene molecule (Scheme 1) preferentially coordinates to four TM^{II} (TM = transition metal) ions, especially for Mn, Fe, Co, or Ni, by their lower-rim phenoxy oxygen and bridge atoms simultaneously forming shuttlecock-like TM_4−calix[4]arene entities performing as a good molecular building blocks (MBBs), which can be bridged by other linkers, including ancillary ligands and bridging anions, into high-nuclearity coordination nanocages.[9] For instance, they can be linked into isolated tetrahedral Co_{16} coordination nanocages with 5-sulfoisophthalates,[9a] octahedral Co_{24} nanocages with di/tricarboxylates,[9b−e] distorted octahedral Mn_{24} nanocage with μ_5-CO_3^{2-} anions,[9f] tetragonal-

Received: March 18, 2014
Revised: April 18, 2014
Published: April 25, 2014

Scheme 1. Structures of Ligands Used in This Paper

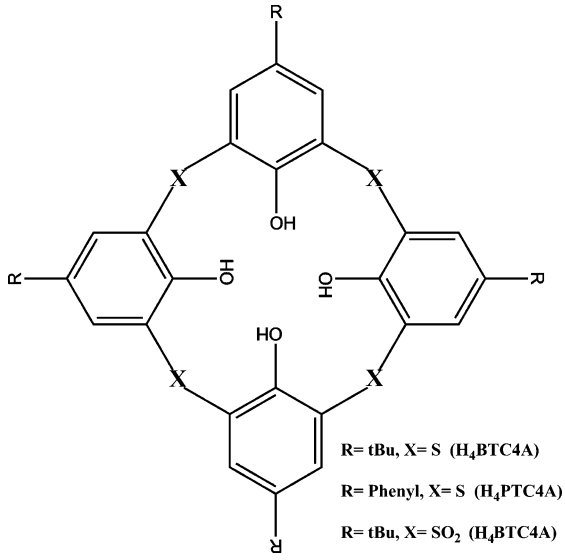

prismatic Co_{32} nanocages by in situ generated 1,3-bis(2*H*-tetrazol-5-yl)benzene ligands,[9g] and two-dimensional metal−calixarene polymers comprising predesigned M_{12} (M = Fe, Co) nanocages with isonicotinates.[9h] Moreover, the TM_4−calix[4]-arene MBBs can be also bridged into other isolated polymetallic clusters including nanospheres, metallamacrocycles, barrels, and other fascinating structures.[10]

A second family of ligands widely utilized in the construction of polymetallic coordination complexes are phosphate and phosphonate ligands, which possess different anionic forms and thus can adopt various coordination modes to bind up to different metal ions.[11] With a detailed search in the literature, there is a plethora of phosphate-/phosphonate-based coordination cage complexes with a range of different nuclearities.[12] In addition, phosphate and phosphonate ligands have also been employed to make 1−3 D extended coordination complexes with interesting structures and properties.[13]

For the reasons above, and in addition to the fact that we have communicated a novel open helmet-like Co_{20} (**7**) coordination nanocage assembled by Co_4−calix[4]arene MBBs with in situ generated phosphate ligands very recently,[14] we have tried to extend our research on using different kinds of calix[4]arens with phosphate or phosphonate ligands to prepare polymetallic compounds. Fortunately, we have obtained another seven new calixarene-based nanocages constructed by bridging M_4−calix[4]arene MBBs with phosphate or phosphonate ligands. The molecular formulas for these coordination nanocages are as follows: $[Ni_8(BTC4A)_2(O_3PPh)_2(\mu\text{-}HCOO)_4(DMF)_2(CH_3OH)_2]\cdot 2H_2O\cdot 2dma$ (**1**), $[Ni_8(PTC4A)_2(PO_4)_2(\mu\text{-}HCOO)_4(dma)_4]\cdot 2Hdma\cdot 2H_2O\cdot 2CH_3OH$ (**2**), $[Na_2Ni_{12}(PTC4A)_3(O_3PPh)_6(\mu\text{-}H_2O)(\mu\text{-}Cl)_2]\cdot 4DMF\cdot CH_3OH$ (**3**), $[Na_2Co_{12}(PTC4A)_3(O_3PPh)_6(\mu\text{-}H_2O)(\mu\text{-}Cl)_2]\cdot 3DMF\cdot CH_3OH$ (**4**), $[Na_4Ni_{16}BSC4A)_4(O_3PPh)_8(\mu_4\text{-}OH)_4(CH_3OH)_4]$ (**5**), $[Na_4Co_{16}(BSC4A)_4(O_3PPh)_8(\mu_4\text{-}OH)_4(CH_3OH)_4]$ (**6**), $[Co_{20}(BTC4A)_5(\mu\text{-}H_2O)(\mu_3\text{-}OH)_4(HPO_4)_8]\cdot DMF\cdot 4CH_3OH$ (**7**), $[Co_{24}(BTC4A)_6(PO_4)_8(\mu_4\text{-}Cl)_6]\cdot 6Hdma\cdot H_2O$ (**8**) (H_4BTC4A = *p-tert*-butylthiacalix[4]arene; H_4PTC4A = *p*-phenylthiacalix[4]-arene; H_4BSC4A = *p-tert*-butylsulfonylcalix[4]arene; DMF = *N*,*N*′-dimethylformamide; dma = dimethylamine; Hdma = dimethylamine cation). Herein, the preparations, crystal structures and properties of compounds **1**−**8** are presented and discussed.

EXPERIMENTAL SECTION

Materials and Measurements. Starting materials, *p-tert*-butylthiacalix[4]arene, *p*-phenylthiacalix[4]arene, and *p-tert*-butylsulfonylcalix[4]arene, were prepared according to literature method,[15] while other chemicals and solvents were of reagent grade and purchased from commercial sources and used as received. Elemental analyses (C, H, N) were performed on a German Elementary Varil EL III service. Infrared spectra were recorded in the solid state (KBr pellets) on a Magna 750 FT-IR spectrometer in the 400−4000 cm^{-1} range. Powder X-ray diffraction (PXRD) measurements were recorded at room temperature by a Rigaku-DMAX 2500 X-ray diffractometer for Cu Kα radiation (λ = 0.154 Å). Thermogravimetric analysis (TGA) curves were performed under a N_2 flow by using a Netzsch STA 449C thermal analyzer. Temperature dependence of solid-state direct current (dc) magnetic susceptibilities data were collected from 300 K down to 2 K on microcrystalline sample with a Quantum Design PPMS-9T and MPMS-XL magnetometers. All experimental magnetic data were applied for the diamagnetic corrections of the sample holders and of the constituent atoms according to the Pascal's constants. Moreover, gas adsorption measurements of **7** were carried out in an ASAP 2020 surface area analyzer.

Synthesis Procedures. *Compound 1*. H_4BTC4A (0.1 mmol, 72 mg), $NiCl_2\cdot 6H_2O$ (0.4 mmol, 95 mg), and $PhPO_3H_2$ (0.1 mmol, 16 mg) were taken in 10 mL of DMF-CH_3OH (v/v 1:1). The mixture was sealed in a 25 mL Teflon-lined bomb at 150 °C for 120 h and then cooled slowly to room temperature for 24 h. X-ray quality crystals were isolated by filtration, washed with DMF/CH_3OH (1:1, v/v), and air-dried. Yield 48% based on ligand. Elemental analysis (%) calculated for **1**: C, 47.48; H, 5.24; N, 2.05. Found C, 46.98; H, 5.27; N, 1.98. IR (KBr disk, ν/cm^{-1}): 3410 (w), 3280 (w), 2962 (s), 2864 (m), 2816 (w), 2725 (w),1673 (m), 1595 (s), 1552 (m), 1446 (s), 1385 (m), 1356 (s), 1258 (s), 1144 (w), 1095 (s), 980 (w), 915 (w), 882 (w), 833 (m), 754 (m), 654 (w), 581 (m), 540 (w), 446 (m).

Compound 2. H_4PTC4A (0.1 mmol, 80 mg), $NiCl_2\cdot 6H_2O$ (0.4 mmol, 95 mg), and Na_2HPO_4 (0.1 mmol, 14 mg) were taken in 10 mL of DMF−CH_3OH (v/v 1:1). The mixture was sealed in a 25 mL Teflon-lined bomb at 150 °C for 72 h and then cooled slowly to room temperature for 24 h. X-ray quality crystals were isolated by filtration, washed with DMF/CH_3OH (1:1, v/v) and air-dried. Yield 38% based on ligand. Elemental analysis (%) calculated for **2**: C, 48.79; H, 4.17; N, 2.00. Found C, 48.56; H, 4.22; N, 1.96. IR (KBr disk, ν/cm^{-1}): 3381 (w), 3247 (w), 3027 (w), 2945 (w), 2831 (w), 1665 (m), 1596 (s), 1445 (s), 1380 (m), 1310 (m), 1257 (s), 1095 (m), 1021 (m), 948 (w), 914 (w), 874 (w), 760 (s), 695 (m), 605 (s), 516 (w), 434 (m).

Compound 3. H_4PTC4A (0.1 mmol, 80 mg), $NiCl_2\cdot 6H_2O$ (0.4 mmol, 95 mg), $PhPO_3H_2$ (0.2 mmol, 32 mg), and NaOH (0.2 mmol, 8 mg) were taken in 10 mL of DMF−CH_3OH (v/v 1:1). The mixture was sealed in a 25 mL Teflon-lined bomb at 150 °C for 120 h and then cooled slowly to room temperature for 24 h. X-ray quality crystals were isolated by filtration, washed with DMF/CH_3OH (1:1, v/v), and air-dried. Yield 55% based on ligand. Elemental analysis (%) calculated for **3**: C, 51.62; H, 3.32; N, 1.25. Found C, 52.11; H, 3.27; N, 1.19. IR (KBr disk, ν/cm^{-1}): 3557 (w), 3418 (w), 3065 (w), 3027 (w), 1665 (m), 1593 (m), 1469 (s), 1330 (w), 1250 (m), 1127 (s), 1054 (s), 956 (m), 882 (w), 914 (w), 760 (m), 719 (w), 695 (m), 621 (m), 588 (w), 523 (w).

Compound 4. Synthesis as for **3**, except $CoCl_2\cdot 6H_2O$ (0.4 mmol, 95 mg) was used in place of $NiCl_2\cdot 6H_2O$ (0.4 mmol, 95 mg). Yield 57% based on ligand. Elemental analysis (%) calculated for **4**: C, 51.62; H, 3.21; N, 0.95. Found C, 52.33; H, 3.25; N, 0.98. IR (KBr disk, ν/cm^{-1}): 3570 (w), 3415 (w), 3066 (w), 3025 (w), 1668 (m), 1592 (m), 1468 (s), 1332 (w), 1252 (m), 1127 (s), 1060 (s), 957 (m), 884 (w), 915 (w), 760 (m), 720 (w), 688 (m), 622 (m), 588 (w), 515 (w), 472(w).

dx.doi.org/10.1021/cg5003836 | *Cryst. Growth Des.* 2014, 14, 3116−3123

Table 1. Crystallographic Data and Refinement Parameters for Compounds 1−8

	1	2	3	4	5	6	7	8
formula	$C_{108}H_{142}N_4O_{28}P_2S_8Ni_8$	$C_{114}H_{116}N_6O_{28}P_2S_8Ni_8$	$C_{193}H_{148}O_{36}N_4P_6S_{12}Cl_2Na_2Ni_{12}$	$C_{190}H_{141}O_{35}N_3P_6S_{12}Cl_2Na_2Co_{12}$	$C_{212}H_{236}O_{80}P_8S_{16}Na_4Ni_{16}$	$C_{212}H_{236}O_{80}P_8S_{16}Na_4Co_{16}$	$C_{207}H_{257}NO_{62}P_8S_{20}Co_{20}$	$C_{252}H_{314}N_6O_{57}P_8S_{24}Co_{24}$
formula wt	2732.13	2806.18	4491.08	4420.91	5855.98	5859.87	5744.67	6983.72
cryst syst	triclinic	triclinic	monoclinic	monoclinic	tetragonal	tetragonal	triclinic	orthorhombic
space group	$P\bar{1}$	$P\bar{1}$	$C2/c$	$C2/c$	$I4_1/acd$	$I4_1/acd$	$P\bar{1}$	$Cmca$
a (Å)	12.519(7)	12.304(6)	24.549(4)	24.017(6)	30.8006(3)	31.0238(4)	26.2994	40.933(6)
b (Å)	13.070(6)	12.449(6)	28.856(4)	28.969(7)	30.8006(3)	31.0238(4)	33.3014	25.607(4)
c (Å)	21.49(1)	21.12(1)	31.942(5)	31.279(8)	63.5696(12)	63.891(2)	37.9859	35.165(5)
α (deg)	73.36 (1)	84.21(2)	90	90	90	90	79.778	90
β (deg)	89.78(1)	78.95(1)	93.539(2)	95.079(5)	90	90	85.964	90
γ (deg)	70.86(1)	75.88(1)	90	90	90	90	66.865	90
V (Å^3)	3164(3)	3073(3)	22584(6)	21676(9)	60308(1)	61494(2)	30107.34	36858(9)
T/K	293(2)	293(2)	120(2)	120(2)	120(2)	120(2)	100 (2)	120(2)
Z	1	1	4	4	8	8	4	4
R_{int}	0.0436	0.0333	0.0497	0.0560	0.0564	0.0525	0.0455	0.0771
data collected	20628	25940	93381	85368	25092	195420	111143	113298
unique data	10990	10735	19679	24250	17256	13533	73004	1 448
GOF on F^2	1.083	1.037	1.040	1.046	1.065	1.074	1.063	1.051
$R_1{}^a$ $[I > 2\sigma(I)]$	0.0728	0.0700	0.0624	0.0654	0.0723	0.0715	0.0934	0.0853
$wR_2{}^b$	0.1861	0.1897	0.2008	0.1874	0.2183	0.2107	0.2757	0.2413
CCDC NO.	989443	989444	989445	989446	989447	989448	958793	989 49

$^aR_1 = \sum||F_o| - |F_c||/\sum|F_o|$. $^bwR_2 = \{\sum[w(F_o^2 - F_c^2)^2]/\sum[w(F_o^2)^2]\}^{1/2}$

Compound **5**. H_4BSC4A (0.1 mmol, 85 mg), Ni(acac)$_2$ (0.3 mmol, 77 mg, acac = acetylacetonate), $PhPO_3H_2$ (0.1 mmol, 16 mg), and NaOH (0.2 mmol, 8 mg) were taken in 10 mL of CH_3OH. The mixture was sealed in a 25 mL Teflon-lined autoclave at 130 °C for 72 h and then cooled slowly to room temperature for 24 h. X-ray quality crystals were isolated by filtration, washed with CH_3OH and air-dried. Yield 65% based on nickel. Elemental analysis (%) calculated for **5**: C, 43.48; H, 4.06. Found (after dried in vacuum): C, 43.05; H, 4.01. IR (KBr disk, ν/cm^{-1}): 3664 (w), 3598 (w), 3451 (w), 3272 (w), 3060 (w), 2962 (s), 2866 (w), 1836 (w), 1608 (s), 1495 (s), 1363 (m), 1298 (m), 1265 (s), 1218 (s), 1134 (s), 1086 (s), 989 (s), 907 (m), 841 (m), 793 (s), 744 (m), 695 (m), 630 (s), 566 (s), 491 (m).

Compound **6**. Synthesis as for **5**, except Co(acac)$_2$ (0.3 mmol, 77 mg) was used in place of Ni(acac)$_2$. Yield 71% based on cobalt. Elemental analysis (%) calculated for **6**: C, 43.45; H, 4.06. Found (after dried in vacuum): C, 42.97; H, 4.02. IR (KBr disk, ν/cm^{-1}): 3663 (w), 3598 (w), 3427 (m), 3066 (w), 2962 (s), 2868 (w), 1836 (w), 1608 (s), 1495 (s), 1363 (m), 1261 (s), 1216 (w), 1134 (s), 1082 (s), 988 (m), 906 (m), 841 (w), 791 (s), 743 (m), 695 (w), 629 (s), 564 (s), 491 (w).

Compound **7**. H_4BTC4A (0.1 mmol, 72 mg), Co(ClO$_4$)$_2$·6H$_2$O (0.3 mmol, 100 mg), and H_2PO_3 (0.2 mmol, 17 mg) were taken in 10 mL of DMF−CH_3OH (v/v 1:1). The mixture was sealed in a 25 mL Teflon-lined autoclave at 160 °C for 72 h and then cooled slowly to room temperature for 24 h. X-ray quality crystals were isolated by filtration, washed with DMF/CH_3OH (1:1, v/v), and air-dried. Yield 53% based on cobalt. Elemental analysis (%) calculated for **7**: C, 42.72; H, 4.45; N, 2.41. found C, 42.95; H, 4.71; N, 2.28. IR (KBr disk, ν cm^{-1}): 3647 (w), 3427 (m), 2958 (s), 2896 (m), 2864 (m), 1619 (s), 2382 (w), 1682 (s), 1592 (m), 1469 (s), 1396 (m), 1361 (m), 1312 (s), 1265 (s), 1151 (s), 1090 (s), 988 (w), 890 (m), 841 (m), 743 (m), 670 (w), 605 (m), 540 (m), 458 (m).

Compound **8**. H_4BTC4A (0.1 mmol, 72 mg), Co(NO$_3$)2·6H$_2$O (0.4 mmol, 120 mg), and Na_2HPO_4 (0.15 mmol, 21 mg) were taken in 10 mL of DMA−CH_3OH (v/v 1:1) and concentrated HCl (0.25 mL). This mixture was sealed in a 25 mL Teflon-lined autoclave at 160 °C for 72 h and then cooled slowly to room temperature for 24 h. X-ray quality crystals were isolated by filtration, washed with DMA/CH_3OH (1:1, v/v), and air-dried. Yield 66% based on ligand. Elemental analysis (%) calculated for **8**: C, 43.34; H, 4.53; N, 1.20. Found C, 44.02; H, 4.58; N, 1.17. IR (KBr disk, ν/cm^{-1}): 3589 (w), 3427 (m), 2962 (s), 2864 (m), 2354 (w), 1641 (m), 1599 (m), 1470 (s), 1366 (m), 1306 (m), 1265 (s), 1062 (m), 1004 (s), 956 (m), 882 (w), 841 (m), 744 (m), 670 (w), 605 (m), 540 (w), 499 (w), 458 (m).

X-ray Data Collection and Structure Determination. All X-ray single crystal data for compounds **1**−**8** were collected on diffractometers equipped with graphite monochromated Mo Kα radiation (λ = 0.71073 Å), compounds **1** and **2** on a Saturn 70 charge-coupled-device diffractometer at 293 K, **3**−**6** and **8** on a Rigaku Saturn 724+ CCD MicroMax 007 CCD diffractometer at 120 K, and **7** on a SuperNova Dual wavelength diffractometer with an Atlas CCD detector at 100 K. The CrystalClear program was applied for the absorption correction.[16] All crystal structures were solved by direct methods and refined using full-matrix least-squares on F^2 by the SHELXTL-97 program package.[17] All the non-hydrogen atoms were refined anisotropically except some got badly disordered atoms and the lattice solvent molecules. Hydrogen atoms of the organic ligands were generated theoretically onto the specific atoms and refined isotropically with fixed thermal factors. Moreover, diffuse electron density associated with solvent molecules in void spaces of the nanocages and hydrogen atoms on some coordinated water and solvent molecules cannot be generated due to disorder and weak crystal diffraction, but they were directly added into the molecular formulas. Because the crystals do not diffract very well owing to the weak crystal diffractions and structure disorder, the R_1 and wR_2 factors in the final structure refinement are relatively high, but typical in such system. Therefore, the "SQUEEZE" method routine in PLATON was applied for the crystal structures of compounds **3**−**8**, which had dramatically improved the agreement indices. The summary of crystallographic data and structure refinement details for compounds **1**−**8** are summarized in Table 1.

RESULTS AND DISCUSSION

Syntheses and General Coordination Nanocage Construction Analysis. All eight crystal structural features are based on shuttlecock-like M$_4$−calix[4]arene MBBs (M = Ni or Co), where M$_4$ cluster cores are capped by cone-shaped

dx.doi.org/10.1021/cg5003836 | Cryst. Growth Des. 2014, 14, 3116−3123

calix[4]arene ($BTC4A^{4-}$, $PTC4A^{4-}$, or $BSC4A^{4-}$) ligands with four phenolic oxygen atoms, four bridge atoms and a cork base at the lower rim as vertices, and phosphonate or phosphate ligands as linkers. However, the shapes of the M_4 quadrangular clusters are somewhat different and the cork bases in the lower-rim of the M_4–calix[4]arene MBBs such as μ_4-OH, μ_2-Cl, μ_4-Cl, and so on are also different. Notably, phosphonate ligand in **1** and phosphate ligand in **2** not only work as the linkers but also as the cork bases, which are distinct from the other six compounds. Moreover, the oxidation states of nickel and cobalt ions (at +2 states) and the protonation levels of all oxygen atoms in these compounds are confirmed by metal and oxygen bond valence sum calculations (BVS), bond lengths, and charge balance. The phosphate ligand with four donor oxygen atoms while phosphonate with three, however, both of above ligands here use three donor oxygen atoms to coordinate one or two metal ions and show five kinds of coordination modes according to Harris notation (Scheme 2).[18] Moreover, all

Scheme 2. Coordination Modes of $PhPO_3^{2-}$, HPO_4^{2-}, and PO_4^{3-} Ligands in This Article, Labeled with Harris Notation

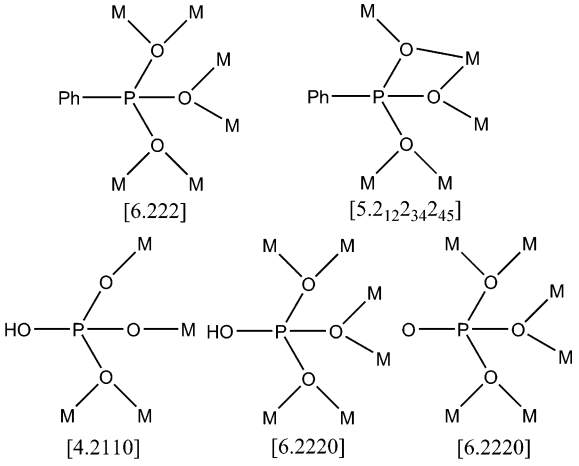

phosphate ligands in **7** carry a hydrogen atom because the separations between the phosphorus and oxygen atoms not coordinating to any metal atom are about 1.585 Å, which are considerably longer than those (being about 1.520 Å) in **2** and **8** and consistent with the presence of P-OH groups. Such is agreed with the previously reported phosphate-based complexes.[19] By virtue of the versatile coordination modes of phosphate and phosphonate ligands, we have systematically prepared a family of high-nuclearity M_{4n} nanocages (M = Ni or Co; n = 2–6) based on three different kinds of M_4–calix[4]arene MBBs. These eight compounds can be divided into five structural types by the number of M_4–calix[4]arene MBBs, including chair-like Ni_8 (**1** and **2**), sphere-shaped M_{12} (**3** and **4**), capsule-like M_{16} (**5** and **6**), helmet-shaped Co_{20} (**7**), and truncated octahedral Co_{24} (**8**) cages (Figure 1). Compounds **1** and **2** are similar to our previous reported Ni_8 compounds, except mainly their μ_6-carbonato ligands are replaced by the μ_6-phosphonate/phosphate ligands in **1** and **2**.[20] Compounds **3**–**6** are unprecedented owing to the fact that they are also linked by sodium ions and present 2p-3d closed-shell heterometallic cage compounds, differing to the homo 3d metallic compounds constructed by three or four M_4–calix[4]arene MBBs.[10c,21] Compound **8** is a closed-shell truncated octahedral Co_{24} cage assembled by six Co_4–

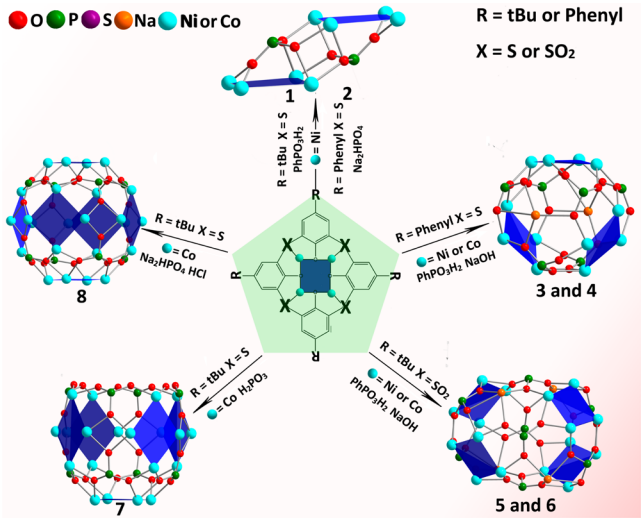

Figure 1. Preparation route of compounds **1**–**8**. Structure of M_4–calix[4]arene MBBs (central). Core structures of **1**–**8**. Calix[4]arene ligands and phenyl groups are omitted for clarity.

calix[4]arene MBBs and eight phosphate ligands, which are similar to the reported Co_{24} cages through a [6 + 8] condensation, while compound **7** is an open pentameric calixarene-based Co_{20} cages, which can be thought of as the truncated octahedral Co_{24} (**8**) nanocage cutting one face. With an increasing in the number of M_4–calix[4]arene MBBs, the inner cavity sizes of the coordination nanocages also increase (Supporting Information Figure S6). For clarity, the detailed structures of **1**–**8** are separately described below.

Crystal Structures. X-ray diffraction studies reveal that compounds **1** and **2** belong to the space group $P\bar{1}$ within triclinic crystal system. These two compounds are structurally analogous, each of which houses a chairlike Ni^{II}_8 core caped by two $BTC4A^{4-}$ ligands (Figure 2a). The main differences

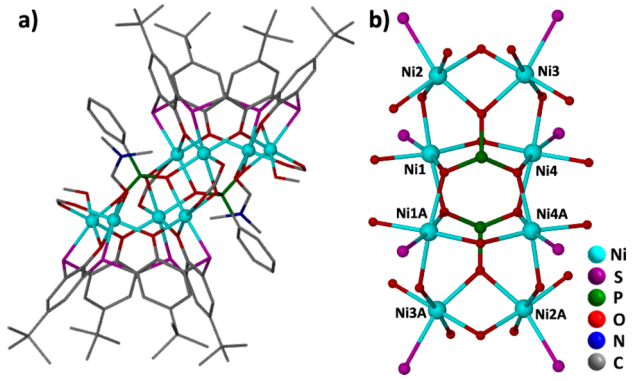

Figure 2. (a) Molecular structure of compound **1**. Hydrogen atoms are omitted for clarity. (b) The chairlike octanuclear Ni^{II}_8 core within compound **1**. Symmetry code: (A) 2 − x, −y, 1 − z.

between them lie in the $BTC4A^{4-}$ and $PhPO_3^{2-}$ ligands in **1** being replaced by $PTC4A^{4-}$ and PO_4^{3-} ligands in **2**. So we only take compound **1** as an example to describe in detail hereafter. There are four crystallographically independent Ni^{II} ions (namely, Ni1–Ni4), and they are all six-coordinated and distorted octahedral in geometry (Figure 2b). Except one O from formate anion, one O from $PhPO_3^{2-}$ ligand, one S, and two phenolic O atoms, the sites Ni1 and Ni2 are still

dx.doi.org/10.1021/cg5003836 | Cryst. Growth Des. 2014, 14, 3116–3123

coordinated by one O from $PhPO_3^{2-}$ ligands, while Ni3 and Ni4 are bonded by one N from dma. These four Ni^{II} ions are bonded by the low-rim phenolic O and bridging S atoms, forming a Ni_4–BTC4A MBB (neighboring Ni···Ni distances ranging from 3.075 to 3.590 Å, and Ni–Ni–Ni angles ranging from 85.21 to 95.55°), which is further connected by two HPO_4^{2-} anions with a [6.2220] coordination mode as well as four formate anions generated from decarbonation of DMF as linkers into a chairlike Ni^{II}_8 entity. Moreover, the distances between the upper and lower adjacent Ni_4–BTC4A MBBs are about 3.192–3.544 Å.

The reaction of H_4PTC4A, $PhPO_3H$, and NaOH with $MCl_2·6H_2O$ (M = Ni or Co) results in the isolation of two 2p-3d heterometallic compounds of sphere-shaped Na_2Ni_{12} (**3**) and Na_2Co_{12} (4). Both crystallize in the monoclinic system with space group *C*2/*c*. These two compounds show similarity in coordination environment, and hence a detailed description of **3** is given here. Compound **3** contains a $Na_2Ni^{II}_{12}$ core, which is built by three M_4–PTC4A MBBs as vertices and six phosphate ligands and two sodium ions as linkers (Figure 3a). Within the

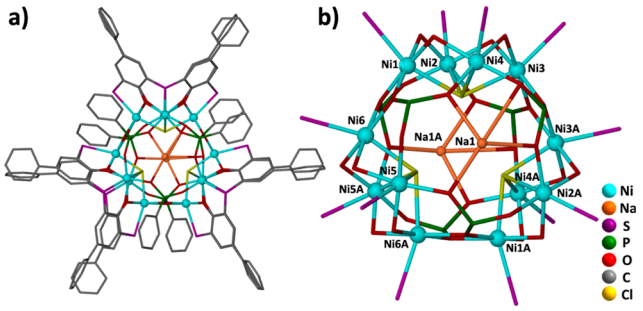

Figure 3. (a) Molecular structure of compound **3**. The hydrogen atoms are omitted for clarity. (b) Representation of the sodium(I) and nickel(II) coordination of **3**.

asymmetric unit of **3**, there is a crystallographically unique sodium ion and six nickel centers (Figure 3b). The former is four-coordinated, with four oxygen atoms from three phosphonate ligands in the same side. The latter can be divided into two groups according to their coordination environment. Ni1, Ni3, and Ni5 are six-coordinated and distorted octahedral in geometry with two phenoxyl O atoms, two O atoms from two different $PhPO_3^{2-}$ ligands, one S atom, and one μ_2-Cl or μ_2-H_2O, while Ni2, Ni4, and Ni6 are five-coordinated in a distorted square pyramid coordination geometry with two phenoxyl O atoms, one S atom, and two O atoms from two different $PhPO_3^{2-}$ ligands. It is to be noted that this coordination nanocage contains a small inner cavity and describes a closed-shell structure because the ports are sealed by two sodium ions. The arrangement of the metal cores in the Ni_4–PTC4A MBBs can seem to be a approximate rhombus shape, with the Ni···Ni separations in the edges being about 3.289 Å and with two groups of inner angles being about 83.6 and 95.8°, respectively. It is noteworthy that the distances between the nickel ions to the sites in the lower-rim of the Ni_4–PTC4A MBBs are longer than the bond distance of Ni–O (2.001(2)–2.194(5) Å) but shorter than the bond distance of Ni–Cl (2.445(2)–2.448(2) Å) because of the site share of Cl and O with the occupancy factor in the molar ratio of 2:1. This ratio is based on the charge-balance consideration and crystallographic analysis. The sodium ion is four-coordinated and bonded by four oxygen atoms from three different $PhPO_3^{2-}$ ligands in the same side. It should be noted that each of the $PhPO_3^{2-}$ ligands binds to five nickel cations with a $[5.2_{12}2_{34}2_{45}]$ chelating mode in this structure. Compared with the saddle-like M_{12} (M = Ni or Co) clusters jointed together by three M_4–PTC4A MBBs and six in situ generated 5-methyl tetrazolate ligands, the aforementioned two compounds feature closed-shell $Na_2M^{II}_{12}$ cages.[21] This is mainly ascribed to the auxiliary ligands, which play different linking modes in them as well as the sodium ions.

Solvothermal treatment of H_4BSC4A with $PhPO_3H_2$, NaOH, and $M(ClO_4)_2·6H_2O$ (M = Ni or Co) in methanol solution affords large X-ray suitable nanocages with capsule-liked Na_4Ni_{16} (**5**) or Na_4Co_{16} (**6**). They are isostructural and crystallize in the orthorhombic *I*41/*acd* space, and thus compound **5** is described in detail as an example hereafter. The Na_4Ni_{16} core is constructed by four Ni_4–TBCS4A MBBs, eight phosphonate ligands and four sodium cations as linkers, and has a crystallographic 4-fold axis so that there are one Na^+ and four Ni^{II} crystallographically unique sites in each asymmetry unit (Figure 4). Each Ni^{II} site is coordinated by

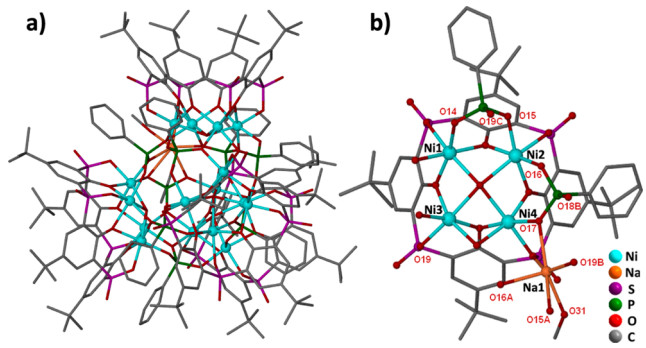

Figure 4. (a) Molecular structure of compound **5**. (b) X-ray asymmetric unit of **5**. Symmetry codes: A 1/4 + –, 7/4 – *x*, 1/4 – *z*; B 7/4 – *y*, *x* – 1/4, 1/4 – *z*; C 2 – –, 3/2 – y, z. The hydrogen atoms are omitted for clarity.

six O atoms, which are arranged in the vertexes of distorted octahedron geometry with two phenoxyl oxygen atoms, one sulfonyl O atom, one μ_4-OH, and two O atoms from two different $PhPO_3^{2-}$ ligands. The sodium ions coordinate to six O atoms, four from three $PhPO_3^{2-}$ ligands, one from $TBCS4A^-$ ligand as well as one from terminal MeOH, so it blocks the window of this nanocage, leading to a closed-shell structure. In each quadrangular Ni_4 core, it is found that the neighboring Ni3···Ni4 separation is 2.724 Å, which is shorter than other three (Ni1···Ni2 3.036 Å, Ni2···Ni3 3.022 Å, Ni1···Ni4 3.008 Å). Moreover, the interior angles of the Co4 core are in the range of 86.12–93.67°. After a close inspection, it is found that eight phosphate ligands adopt two different coordination modes, with half in [6.222] and the other half in $[5.2_{12}2_{34}2_{45}]$ in coordination modes. Although there is a report on metal–organic supercontainers constructed by four MBBs, those M_4–TBCS4A (M = Ni or Co) MBBs here are linked by eight dicarboxylates, leading to a barrel shape.[10c]

For clarity, we will describe the truncated octahedral nanocage Co_{24} (**8**) first, because the open Co_{20} nanocage (**7**) can be regard as a truncated octahedral Co_{24} cage cutting one face. Single-crystal X-ray diffraction analysis reveals that compound **8** crystallizes in the orthorhombic space group *Cmca*, featuring an anionic nanosized coordination cage (Figure 5a). The essential feature of **8** possesses a truncated octahedral

dx.doi.org/10.1021/cg5003836 | *Cryst. Growth Des.* 2014, 14, 3116–3123

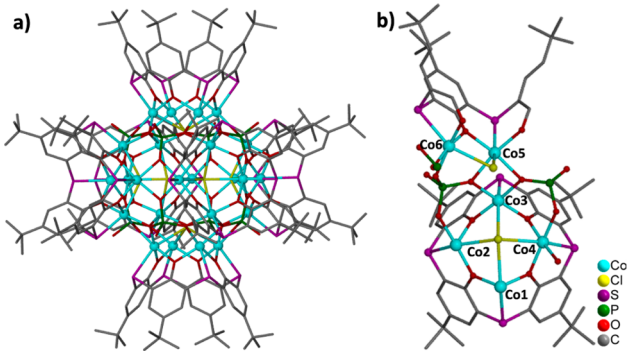

Figure 5. (a) Molecular structure of compound **5**. The hydrogen atoms are omitted for clarity. (b) X-ray asymmetric unit of **5**.

coordination cage composed of six Co_4–TBC4A MBBs acting as the faces and eight phosphate anions as linkers. There are six crystallographically independent Co^{II} sites. All Co^{II} ions are six-coordinated in distorted octahedron geometries, and each site is coordinated by two phenoxyl O atoms, one S atom, one μ_4-Cl, and two O atoms from two different PO_4^{3-} anions (Figure 5b). Structural analysis shows that the Co_4 core in this structure describes to be a approximate square shape, with the Co···Co separations for the edge ranging from 3.249 to 3.259 Å and with the inner angles ranging from 89.80° from 90.15°. Every PO_4^{3-} anion binds to six cobalt cations with the same [6.2220] chelating mode. It should be noted that compound **8** is quite similar to the reported $Co^{II}_{24}M^{VI}_8$ (M = Mo, W)[22] and Co^{II}_{32} nanospheres[23] except the bridging PO_4^{3-} sites are replaced by the $M^{VI}O_4$ and $Co^{II}O_6$ sites, respectively. However, nanocage Co_{24} (**8**) is different from the reported hexameric calix[4]arene-based Co_{24} nanocages through a [6 + 8] condensation by tripodal aromatic carboxylic acids because this Co_{24} nanocage has a small inner cavity and no port at all edges of the truncated octahedron.[9b−d] Such is due to the phosphate ligands being much smaller than those tripodal aromatic carboxylate ligands.

With H_4BTC4A, phosphorous acid, and cobalt(II) perchlorate hexahydrate, an icosanuclear compound $[Co_{20}(BTC4A)_5(\mu_2\text{-}H_2O)(\mu_3\text{-}OH)_4(HPO_4)_8]_2\cdot DMF\cdot 4CH_3OH]$ (**7**) results (Figure 6), previously communicated.

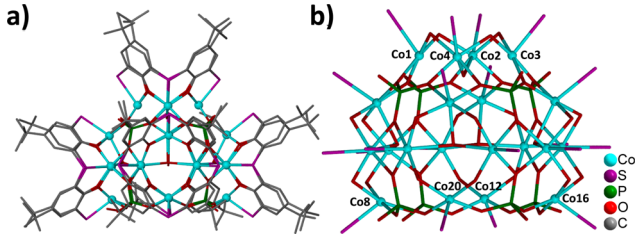

Figure 6. (a) Helmet-like molecular structure of compound **7**. The Hydrogen atoms are omitted for clarity. (b) Icosanuclear Co_{20} core within compound **7**.

Compared with the structure of Co_{24} nanocage (**8**), this helmet-like nanocage Co_{20} (**7**) can be thought to form by cutting one face of the truncated octahedron. Thus, compound **7** has an opening, which shows a 16-membered ring with repeat –[Co–O–P-O]– units, and its diameter (opposed Co···Co distance) is ∼8.758 Å (Supporting Information Figure S2). Moreover, this Co_{20} open nanocage has an inner cavity with the volume being ∼380 $Å^3$, which is much smaller than the reported octahedral Co_{24} nanocages linked by aromatic carboxylates.[9b−e] It should be pointed out that compound **7** is the only one in this family with an open-shell structure. Thus, the gas sorption isotherms of **7** have been measured to confirm the architecture rigidity and permanent porosity (Supporting Information Figure S3). The calculated Brunauer–Emmett–Teller (BET) and Langmuir apparent surface areas are 388 and 579m^2 g^{-1}, respectively. Moreover, compound **7** is in triclinic space group $P\bar{1}$, of which asymmetric unit is large and contains two of the formulas.

The Co_{20} coordination cage is assembled by five Co_4–TBC4A MBBs and eight HPO_4^{2-} anions. The five Co_4–TBC4A MBBs in this structure can be divided into two types according to the difference in cobalt bonding modes: the upper Co_4–TBC4A MBB (including Co1, Co2, Co3, and Co4) in the helmet adopts an approximate rhombus shape with a μ_2-H_2O in its lower rim, while the Co_4 clusters in the left four MBBs, showing similarity in the coordination environment, adopt an approximate kite-like shape and house a μ_3-OH (Supporting Information Figure S4). It should be noted that all eight HPO_4^{2-} ligands in **7** are originated from an in situ reaction of H_2PO_3, and show two binding modes: four in the lower part of the helmet with [4.2110] binding mode, while the rest show [6.2220] mode.

Magnetic Properties. The variable-temperature direct current (dc) magnetic susceptibilities of the four nickel–calixarene compounds (**1**–**3** and **5**) are performed on polycrystalline samples over 2–300 K and under a magnetic field of 1 kOe (Figure 7a). The $\chi_m T$ values at room temperature are 7.67, 7.78, 11.64, and 15.69 cm^3 K mol^{-1} for **1**–**3** and **5**, respectively, which are closed to the expected values of 8 (8.00 cm^3 K mol^{-1}), 12 (12.00 cm^3 K mol^{-1}), or 16 (16.00 cm^3 K

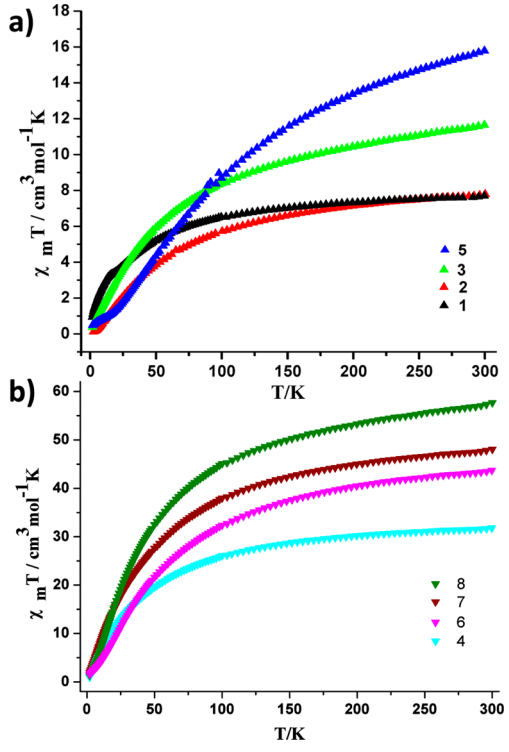

Figure 7. (a) Temperature dependence of magnetic susceptibilities of compounds **1**–**3** and **5** in a 1000 Oe field. (b) Temperature dependence of magnetic susceptibilities of compounds **4** and **6**–**8** in a 1000 Oe field.

dx.doi.org/10.1021/cg5003836 | Cryst. Growth Des. 2014, 14, 3116–3123

mol^{-1}) for isolated Ni^{II} ions. Upon cooling, all four $\chi_m T$ values decrease continuously to low temperatures, but that of **5** is more rapidly than those of **1**−**3** in the high temperature region. The reciprocal molar magnetic susceptibilities data obey the Curie−Weiss law ($1/\chi_m = T/C - \theta/C$) in the range of 50−300 K with Curie constants of C = 8.45, 9.59, 14.20 cm^3 K mol^{-1}, and Weiss constants of θ = −30.63, −68.90, and −70.60 K for **1**−**3**, respectively, and fitting the magnetic of **5** above 100 K to the law gives C = 17.06 cm^3 K mol^{-1} and θ = −124.57 K (Supporting Information Figure S5). The negative value of the Weiss temperature, together with the curve of $\chi_m T$ (T), indicates the presence of non-negligible antiferromagnetic (AF) coupling between Ni^{II} ions. However, the coupling parameters (J) are not be able to determine because the complexity of these four structures and thus there are too many J values.

Magnetic susceptibility measurements of the other four cobalt−calixarene compounds (**4** and **6**−**8**) are also carried out on the polycrystalline samples in the temperature range of 2−300 K with a 1 kOe applied field (Figure 7b). The room temperature $\chi_m T$ values are 31.77, 43.71, 48.07, and 57.67 cm^3 K mol^{-1} for compounds **4** and **6**−**8**, respectively, which are significantly higher than the calculated value of 12 (22.25 cm^3 K mol^{-1}), 16 (30.00 cm^3 K mol^{-1}), 20 (37.50 cm^3 K mol^{-1}), or 24 (45.00 cm^3 K mol^{-1}) for uncoupled Co(II) spin carriers. This can be ascribed to the unquenched orbital-moment as a consequence of spin−orbital coupling of Co^{II} ions, which is known to be significant in an octahedral field.[24] For all these four compounds, the $\chi_m T$ products gradually decrease and then fall rapidly to low temperatures. The Curie−Weiss law fit of the data above 50 K gives the Curie constant C = 36.10, 43.47, and 52.67, 66.84 cm^3 mol^{-1} K and Weiss constant θ = −39.71, −49.64, −45.65, and −50.30 K for **4** and **6**−**8** (Supporting Information Figure S6), respectively. The negative Weiss constants and the gradual decline of $\chi_m T$ values at higher temperatures may be due to the presence of intramolecular antiferromagnetic interaction and/or the spin−orbit coupling effect of Co^{II} ions in the clusters.

CONCLUSION

In summary, we have successfully systematically synthesized eight high-nuclearity discrete nanocages constructed from M_4−calix[4]arene MBBs with inorganic phosphate or organic phosphonate linkers. By virtue of the different coordination modes of phosphate or phosphonate ligands, initial reactions combining them with in situ generated M_4−calix[4]arene MBBs have produced chairlike Ni_8 (**1** and **2**), sphere-shaped M_{12} (**3** and **4**), capsule-like M_{16} (**5** and **6**), helmet-like Co_{20} (**7**), and truncated octahedral Co_{24} (**8**) coordination nanocages. This work sheds some light into the design and synthesis of high-nuclearity cage-like compounds with the multidentate complementary ligands and also profoundly improves our understanding on the correlation between the M_4−calix[4]-arene MBBs and their cage-like structures. Future efforts will focus on utilizing multifunctional phosphonate ligands or other metals in the synthesis of polymetallic 3d, 4f, or 3d-4f coordination complexes with interesting structures and properties.

ASSOCIATED CONTENT

Supporting Information

X-ray structural data in CIF format (CCDC 989443−989449 and 958793), TGA analyses and PXRD patterns for compounds **1**−**8**, and other additional pictures and data. This material is available free of charge via the Internet at http://pubs.acs.org.

AUTHOR INFORMATION

Corresponding Author

*E-mail: mchong@fjirsm.ac.cn.

Notes

The authors declare no competing financial interest.

ACKNOWLEDGMENTS

We thank Special Project of National Major Scientific Equipment Development of China (2012YQ120060), and Deanship of Scientific Research (DSR), King Abdulaziz University, Jeddah, under grant number (1-130-1434-HiCi) for funding this research.

REFERENCES

(1) (a) Osuga, T.; Murase, T.; Ono, K.; Yamauchi, Y.; Fujita, M. *J. Am. Chem. Soc.* **2010**, *132*, 15553−15555. (b) Wu, B.; Cui, F.; Lei, Y.; Li, S.; de Sousa Amadeu, N.; Janiak, C.; Lin, Y.-J.; Weng, L.-H.; Wang, Y.-Y.; Yang, X.-J. *Angew. Chem., Int. Ed.* **2013**, *52*, 5096−5100. (c) Zhou, X. P.; Wu, Y.; Li, D. *J. Am. Chem. Soc.* **2013**, *135*, 16062−16065. (d) Custelcean, R. *Chem. Soc. Rev.* **2014**, *43*, 1813−1824.

(2) (a) Sudik, A. C.; Millward, A. R.; Ockwig, N. W.; Côté, A. P.; Kim, J.; Yaghi, O. M. *J. Am. Chem. Soc.* **2005**, *127*, 7110−7118. (b) Qian, J.; Jiang, F.; Zhang, L.; Su, K.; Pan, J.; Li, Q.; Yuan, D.; Hong, M. *Chem. Commun.* **2014**, *50*, 1678−1681.

(3) (a) Bilbeisi, R. A.; Ronson, T. K.; Nitschke, J. R. *Angew. Chem., Int. Ed.* **2013**, *52*, 9027−9030. (b) Takezawa, H.; Murase, T.; Fujita, M. *J. Am. Chem. Soc.* **2012**, *134*, 17420−17423.

(4) (a) Murase, T.; Nishijima, Y.; Fujita, M. *J. Am. Chem. Soc.* **2012**, *134*, 162−164. (b) Zhang, Q.; Tiefenbacher, K. *J. Am. Chem. Soc.* **2013**, *135*, 16213−16219.

(5) (a) Zheng, Y.-Z.; Evangelisti, M.; Tuna, F.; Winpenny, R. E. P. *J. Am. Chem. Soc.* **2012**, *134*, 1057−1065. (b) Cameron, J. M.; Newton, G. N.; Busche, C.; Long, D. L.; Oshio, H.; Cronin, L. *Chem. Commun.* **2013**, *49*, 3395−3397.

(6) (a) Clever, G. H.; Kawamura, W.; Tashiro, S.; Shiro, M.; Shionoya, M. *Angew. Chem., Int. Ed.* **2012**, *51*, 2606−2609. (b) Bunzen, J.; Iwasa, J.; Bonakdarzadeh, P.; Numata, E.; Rissanen, K.; Sato, S.; Fujita, M. *Angew. Chem., Int. Ed.* **2012**, *51*, 3161−3163. (c) Chepelin, O.; Ujma, J.; Wu, X.; Slawin, A. M. Z.; Pitak, M. B.; Coles, S. J.; Michel, J.; Jones, A. C.; Barran, P. E.; Lusby, P. J. *J. Am. Chem. Soc.* **2012**, *134*, 19334−19337. (d) Zhang, Q.; Jiang, F.; Huang, Y.; Wu, M.; Hong, M. *Cryst. Growth Des.* **2009**, *9*, 28−31. (e) Chen, L.; Jiang, F. L.; Wu, M. Y.; Li, N.; Xu, W. T.; Yan, C. F.; Yue, C. Y.; Hong, M. C. *Cryst. Growth Des.* **2008**, *8*, 4092−4099. (f) Pang, J.; Jiang, F.; Wu, M.; Yuan, D.; Zhou, K.; Qian, J.; Su, K.; Hong, M. *Chem. Commun.* **2014**, *50*, 2834−2836.

(7) (a) Shanmugam, M.; Chastanet, G.; Mallah, T.; Sessoli, R.; Teat, S. J.; Timco, G. A.; Winpenny, R. E. P. *Chem.—Eur. J.* **2006**, *12*, 8777−8785. (b) Taylor, S. M.; McIntosh, R. D.; Piligkos, S.; Dalgarno, S. J.; Brechin, E. K. *Chem. Commun.* **2012**, *48*, 11190−11192. (c) Zheng, S. T.; Mao, C.; Wu, T.; Lee, S.; Feng, P.; Bu, X. *J. Am. Chem. Soc.* **2012**, *134*, 11936−11939. (d) Aromi, G.; Aguila, D.; Gamez, P.; Luis, F.; Roubeau, O. *Chem. Soc. Rev.* **2012**, *41*, 537−546.

(8) (a) Redshaw, C.; Elsegood, M. R. J.; Wright, J. A.; Baillie-Johnson, H.; Yamato, T.; De Giovanni, S.; Mueller, A. *Chem. Commun.* **2012**, *48*, 1129−1131. (b) Lamouchi, M.; Jeanneau, E.; Novitchi, G.; Luneau, D.; Brioude, A.; Desroches, C. *Inorg. Chem.* **2014**, *53*, 63−72. (c) Fairbairn, R. E.; McLellan, R.; McIntosh, R. D.; Palacios, M. A.; Brechin, E. K.; Dalgarno, S. J. *Dalton Trans.* **2013**, *43*, 5292−5298. (d) Taylor, S. M.; Sanz, S.; McIntosh, R. D.; Beavers, C. M.; Teat, S. J.; Brechin, E. K.; Dalgarno, S. J. *Chem.—Eur. J.* **2012**, *18*, 16014−16022. (e) McLellan, R.; Reze, J.; Taylor, S. M.; McIntosh, R. D.; Brechin, E. K.; Dalgarno, S. J. *Chem. Commun.* **2014**, *50*, 2202−2204. (f) (h) Cholewa, P. P.; Beavers, C. M.; Teat, S. J.; Dalgarno, S. J. *Cryst. Growth*

Des. **2013**, *13*, 5165−5168. (g) Liu, C.-M.; Zhang, D.-Q.; Hao, X.; Zhu, D.-B. *Chem.—Eur. J.* **2011**, *17*, 12285−12288. (h) Su, K.; Jiang, F.; Qian, J.; Zhou, K.; Pang, J.; Basahel, S.; Mokhtar, M.; Thabaiti, S.; Hong, M. *Inorg. Lett.* **2014**, *1* (1), 1−8. (h) Liu, C.-M.; Zhang, D.-Q.; Hao, X.; Zhu, D.-B. *Cryst. Growth Des.* **2012**, *12*, 2948−2954.

(9) (a) Liu, M.; Du, S.; Bi, Y.; Liao, W. *Inorg. Chem. Commun.* **2014**, *41*, 96−99. (b) Liu, M.; Liao, W.; Hu, C.; Du, S.; Zhang, H. *Angew. Chem., Int. Ed.* **2012**, *51*, 1585−1588. (c) Dai, F.-R.; Wang, Z. *J. Am. Chem. Soc.* **2012**, *134*, 8002−8005. (d) Du, S.; Hu, C.; Xiao, J. C.; Tan, H.; Liao, W. *Chem. Commun.* **2012**, *48*, 9177−9179. (e) Xiong, K. C.; Jiang, F. L.; Gai, Y. L.; Yuan, D. Q.; Chen, L.; Wu, M. Y.; Su, K. Z.; Hong, M. C. *Chem. Sci.* **2012**, *3*, 2321−2325. (f) Xiong, K. C.; Jiang, F. L.; Gai, Y. L.; Yuan, D. Q.; Han, D.; Ma, J.; Zhang, S. Q.; Hong, M. C. *Chem.—Eur. J.* **2012**, *18*, 5536−5540. (g) Bi, Y.; Wang, S.; Liu, M.; Du, S.; Liao, W. *Chem. Commun.* **2013**, *49*, 6785−6787. (h) Tan, H.; Du, S.; Bi, Y.; Liao, W. *Chem. Commun.* **2013**, *49*, 8211−8213.

(10) (a) Bi, Y. F.; Wang, X. T.; Liao, W. P.; Wang, X. F.; Wang, X. W.; Zhang, H. J.; Gao, S. *J. Am. Chem. Soc.* **2009**, *131*, 11650−11651. (b) Bi, Y. F.; Xu, G. C.; Liao, W. P.; Du, S. C.; Wang, X. W.; Deng, R. P.; Zhang, H. J.; Gao, S. *Chem. Commun.* **2010**, *46*, 6362−6364. (c) Dai, F.-R.; Becht, D. C.; Wang, Z. *Chem. Commun.* **2014**, *50*, 5385−5387. (d) Xiong, K. C.; Wang, X. Y.; Jiang, F. L.; Gai, Y. L.; Xu, W. T.; Su, K. Z.; Li, X. J.; Yuan, D. Q.; Hong, M. C. *Chem. Commun.* **2012**, *48*, 7456−7458. (e) Su, K. Z.; Jiang, F. L.; Qian, J. J.; Wu, M. Y.; Xiong, K. C.; Gai, Y. L.; Hong, M. C. *Inorg. Chem.* **2013**, *52*, 3780−3786.

(11) (a) Natarajan, S.; Mandal, S. *Angew. Chem., Int. Ed.* **2008**, *47*, 4798−4828. (b) Sheikh, J. A.; Goswami, S.; Adhikary, A.; Konar, S. *Inorg. Chem.* **2013**, *52*, 4127−4129. (c) Chen, Y.; Trzop, E.; Sokolow, J. D.; Coppens, P. *Chem.—Eur. J.* **2013**, *19*, 16651−16655.

(12) (a) Maheswaran, S.; Chastanet, G.; Teat, S. J.; Mallah, T.; Sessoli, R.; Wernsdorfer, W.; Winpenny, R. E. P. *Angew. Chem., Int. Ed.* **2005**, *44*, 5044−5048. (b) Wang, M.; Yuan, D.-Q.; Ma, C.-B.; Yuan, M.-J.; Hu, M.-Q.; Li, N.; Chen, H.; Chen, C.-N.; Liu, Q.-T. *Dalton Trans.* **2010**, *39*, 7276−7285. (c) Zheng, Y.-Z.; Evangelisti, M.; Winpenny, R. E. P. *Angew. Chem., Int. Ed.* **2011**, *50*, 3692−3695. (d) Khanra, S.; Konar, S.; Clearfield, A.; Helliwell, M.; McInnes, E. J. L.; Tolis, E.; Tuna, F.; Winpenny, R. E. P. *Inorg. Chem.* **2009**, *48*, 5338−5349. (e) Ali, S.; Muryn, C. A.; Tuna, F.; Winpenny, R. E. P. *Dalton Trans.* **2010**, *39*, 124−131. (f) Chandrasekhar, V.; Nagarajan, L.; Hossain, S.; Gopal, K.; Ghosh, S.; Verma, S. *Inorg. Chem.* **2012**, *51*, 5605−5616. (g) Langley, S.; Helliwell, M.; Sessoli, R.; Teat, S. J.; Winpenny, R. E. P. *Inorg. Chem.* **2008**, *47*, 497−507.

(13) (a) Mahimaidoss, M. B.; Krasnikov, S. A.; Reck, L.; Onet, C. I.; Breen, J. M.; Zhu, N.; Marzec, B.; Shvets, I. V.; Schmitt, W. *Chem. Commun.* **2014**, *50*, 2265−2267. (b) Perry, H. P.; Gagnon, K. J.; Law, J.; Teat, S.; Clearfield, A. *Dalton Trans.* **2012**, *41*, 3985−3994. (c) Gagnon, K. J.; Perry, H. P.; Clearfield, A. *Chem. Rev.* **2012**, *112*, 1034−1054.

(14) Su, K.; Jiang, F.; Qian, J.; Wu, M.; Gai, Y.; Pan, J.; Yuan, D.; Hong, M. *Inorg. Chem.* **2014**, *53*, 18−20.

(15) (a) Iki, N.; Kabuto, C.; Fukushima, T.; Kumagai, H.; Takeya, H.; Miyanari, S.; Miyashi, T.; Miyano, S. *Tetrahedron* **2000**, *56*, 1437−1443. (b) Lhoták, P.; Šmejkal, T.; Stibor, I.; Havlíček, J.; Tkadlecová, M.; Petříčková, H. *Tetrahedron Lett.* **2003**, *44*, 8093−8097. (c) Morohashi, N.; Iki, N.; Sugawara, A.; Miyano, S. *Tetrahedron* **2001**, *57*, 5557−5563.

(16) *CrystalClear* , version 1.3.6; Rigaku/MSC: 9009 New Trails Drive, The Woodlands, TX 77381−52092004

(17) (a) Sheldrick, G. M. *SHELXL 97, Program for Crystal Structure Refiniement*; University of Göttingen: Göttingen, Germany, 1997. (b) Sheldrick, G. M. *SHELXS 97, Program for Crystal Structure Solution*; University of Göttingen: Göttingen, Germany, 1997.

(18) Coxall, R. A.; Harris, S. G.; Henderson, D. K.; Parsons, S.; Tasker, P. A.; Winpenny, R. E. P. *Dalton Trans.* **2000**, 2349−2356.

(19) Xiong, K. C.; Jiang, F. L.; Gai, Y. L.; Zhou, Y. F.; Yuan, D. Q.; Su, K. Z.; Wang, X. Y.; Hong, M. C. *Inorg. Chem.* **2012**, *51*, 3283−3288.

(20) Cowley, A. R.; Chippindale, A. M. *J. Chem. Soc., Dalton Trans.* **2000**, 3425−3428.

(21) Xiong, K. C.; Jiang, F. L.; Gai, Y. L.; He, Z. Z.; Yuan, D. Q.; Chen, L.; Su, K. Z.; Hong, M. C. *Cryst. Growth Des.* **2012**, *12*, 3335−3341.

(22) Bi, Y. F.; Du, S. C.; Liao, W. P. *Chem. Commun.* **2011**, *47*, 4724−4726.

(23) Gehin, A.; Ferlay, S.; Harrowfield, J. M.; Fenske, D.; Kyritsakas, N.; Hosseini, M. W. *Inorg. Chem.* **2012**, *51*, 5481−5486.

(24) (a) Wang, X. Y.; Gan, L.; Zhang, S. W.; Gao, S. *Inorg. Chem.* **2004**, *43*, 4615−4625. (b) Abu-Youssef, M. A. M.; Mautner, F. A.; Vicente, R. *Inorg. Chem.* **2007**, *46*, 4654−4659.